

Magnetically controlled current flow in coupled-dot arrays

Panagiotis S. Drouvelis,^{1, 2,*} Giorgos Fagas,^{3, †} and Peter Schmelcher^{1, 4, ‡}

¹*Theoretische Chemie, Universität Heidelberg, Im Neuenheimer Feld 229, D-69120 Heidelberg, Germany*

²*Interdisziplinäres Zentrum für Wissenschaftliches Rechnen,
Im Neuenheimer Feld 368, D-69120 Heidelberg, Germany*

³*Tyndall National Institute, Lee Maltings, Prospect Row, Cork, Ireland*

⁴*Physikalisches Institut, Philosophenweg 12, Universität Heidelberg, D-69120 Heidelberg, Germany*

(Dated: December 22, 2019)

Quantum transport through an open periodic array of up to five dots is investigated in the presence of a magnetic field. The device spectrum exhibits clear features of the band structure of the corresponding one-dimensional artificial crystal which evolves with varying field. A significant magnetically controlled current flow with on/off ratios up to many orders of magnitude is induced depending on temperature and material parameters. Our results put forward a simple design for measuring the magnetic subband formation with potential use as an effective magnetoresistance device at very small scales. We discuss possible implementations with current technology.

PACS numbers: 73.23.Ad, 73.21.La, 73.20.At, 73.23.-b

Single quantum dots are the solid state analogue of an atom whereas the properties of coupled-dots may resemble that of molecules. Quantum transport through open quantum dots, being an equally intriguing as well as extensively investigated topic [1], continues to provide new insights in fundamental phenomena and fuels a wealth of nanoelectronic applications. Owing to the high degree of control and access offered to their electronic properties [1, 2, 3], open quantum dots are ideal laboratories for investigating quantum to classical correspondence [4, 5], conductance fluctuations [6], shot noise [7] and phase coherence [8] to name a few examples.

Arrays of coupled-dots may be considered as one-dimensional artificial crystals with the dot repeating unit acting as the lattice basis. If the coupling is strong enough the electronic structure uncovers many similarities with the subbands of quasi one-dimensional systems with a much reduced reciprocal lattice vector. It is also well known that a uniform magnetic field applied to Bloch electrons yields magnetic subbands with an overall different spectrum [9, 10]. Unlike the lack of any impact in one dimension, in two dimensions these form the famous Hofstadter butterfly [11]. The question remains open as to what extent there exists an observable magnetic effect for the intermediate dimensionality, as in the case of an array of open quantum dots. Moreover, experimental evidence in the literature is scarce [12, 13] and the effect of magnetic subbands is hard to isolate in the common setup of lateral semiconductor superlattices [14]. Hence, the prospect of measuring its properties in a simple fashion is quite attractive.

In this Letter we consider small coupled-dot arrays that present distinct spectral properties regulated via an applied magnetic field B . The electron transport exhibits bright and dark windows reflecting an electronic structure that is reminiscent of the energy bands of the corresponding linear artificial crystal. This unique feature

allows to explore the B -dependence of the subbands of the quasi one-dimensional Bloch electrons. With varying magnetic field, our calculations demonstrate qualitative (and quantitative) changes of the bright and dark transport windows in the suggested array structure, thus, yielding a direct signature of the magnetic subband formation in the magnetoconductance.

Coupled-dot arrays may also be used as elements in magnetoresistive devices. For example, by manipulating Fano (anti)resonances single open quantum dots could form such building blocks or, as recently suggested, be applied as spin filters [15]. The array structure allows the formation of wide band gaps. This enables magnetically controlled current flow to change up to few orders of magnitude even at elevated temperatures despite thermal broadening; an additional advantage is the fine tuning allowed by the coupling parameters possibly via back gates. Such a design of chaotic and rectangular quantum dots in alignment has been recently realized with a split-gate technique [7, 16]. In the experiments of Ref. 16 the classical dynamics of the electrons in a magnetic field triggers reflection giving rise to a large magnetoresistance at a field slightly greater than the magnetic field B_c that corresponds to an electron cyclotron radius equal to the size W of the dot, i.e., $B_c = \hbar k_F/eW$ (k_F is the Fermi wavevector). However, we show that the quantum mechanical effect of magnetic subband structure also gives significant magnetoresistance at more moderate fields.

Fig. 1(a) shows the setup in discussion. We assume that square quantum dots of size W are laterally confined on the surface of a semiconductor heterostructure by an electrostatic field which creates effective hard wall boundaries for ballistically propagating electrons. The coupled leads are modelled by quasi one-dimensional conduction band electrons freely propagating along the x -direction with a Fermi distribution $f_K(E) = [\exp(\frac{E-\mu_K}{k_B T}) + 1]^{-1}$, $\mu_K = E_F \pm eV_{SD}/2$ being the chemical potential in the

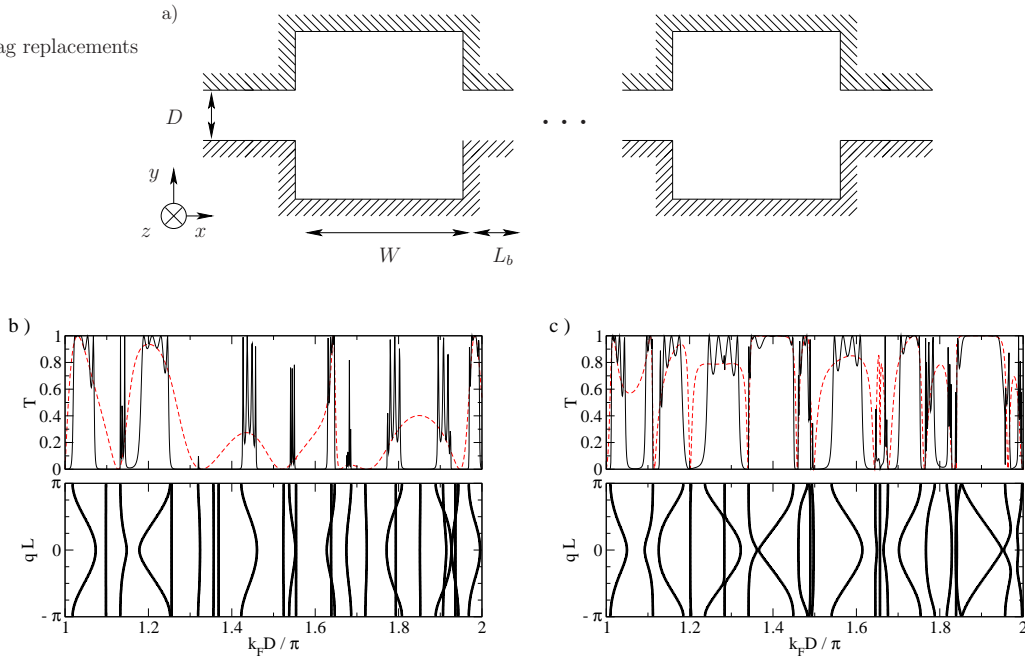


FIG. 1: (Color online) (a) Schematic representation of the discussed open array of quantum dots. (b) Upper panel: field-free quantum transmission through a single-dot (dashed curve) and the five-dot array of (a). Lower panel: energy spectrum of the corresponding one-dimensional artificial crystal with lattice spacing $L = W + L_b$. Note that flat energy bands do not contribute to transport since electrons acquire zero group velocity. (c) Same as (b) for a magnetic flux $\Phi \approx 4.5\phi_0$ piercing the unit cell. We recall that the integer part of $k_F D / \pi$ indicates the number of propagating channels in the leads and q defines the Bloch vector of the periodic structure.

left ($K=L$) and right ($K=R$) lead when a bias voltage V_{SD} is applied. The point contacts bridging the dots have square geometry of dimensions $L_b = D = 0.3W$ that are of the order of the Fermi wavelength $\lambda_F = 2\pi/k_F$. Although quantitative details differ, our main conclusions are independent of this simplest design.

We model the electronic structure via a single-band effective mass equation of electrons in a magnetic field, which when discretized on a lattice, is most easily expressed in the second quantization form

$$H(\mathbf{r}) = \sum_{\mathbf{r}} \epsilon_{\mathbf{r}} c_{\mathbf{r}}^\dagger c_{\mathbf{r}} + \sum_{\mathbf{r}, \Delta\mathbf{r}} (V e^{2\pi i \frac{\mathbf{A}(\mathbf{r}) \Delta\mathbf{r}}{\phi_0}} c_{\mathbf{r}}^\dagger c_{\mathbf{r} + \Delta\mathbf{r}} + h.c.). \quad (1)$$

Here, $\Delta\mathbf{r}$ indicates nearest neighbors to the site \mathbf{r} and the on-site energy is $\epsilon_{\mathbf{r}} = 4V$ with the hopping matrix element $V = \hbar^2/2m^*a^2$; m^* is the effective mass (fixed to $0.05m_e$ unless otherwise stated) and a is our lattice mesh constant. The magnetic field $\mathbf{B} = B\mathbf{z}$ applied to the dot array is introduced via the vector potential \mathbf{A} in the Peierls phase factor; $\phi_0 = h/e$ is the flux quantum. Charge transport properties are calculated within the Landauer scattering-matrix formalism which expresses the current

$$I = \frac{2e}{h} \int_{-\infty}^{\infty} T(E)(f_L(E) - f_R(E))dE \quad (2)$$

through the quantum transmission function $T(E)$ for injected electrons with energy E ; the factor two accounts for spin degeneracy. We calculate T using our recently developed parallel algorithm of the recursive Green's functions method [17]. As the system size increases one needs to invert a block-tridiagonal matrix which scales linearly with the array length. For serial processing this yields an additional cost that we avoid by distributing the scatterer's domain over several processors.

The upper panels of Figs. 1(b) and 1(c) show the field-free and $B \neq 0$, respectively, quantum transmission in the first open channel. Transport through a five-dot array is indicated by the solid curves. In contrast to the single-dot transmission spectrum - plotted in dashed line - bright and dark windows are formed in which transport is either allowed or suppressed. These compare well with the energy bands and gaps of the electronic structure of the corresponding infinite linear artificial lattice shown for zero and finite B in the lower panels of Figs. 1(b) and 1(c), respectively. Also evident in those figures is the prominent dependence of the band structure with respect to the magnetic flux piercing the unit cell. Broad energy bands contribute electron states that are almost fully transmitted, whereas, narrow sections exhibit weaker transmission signals. The remarkable characteristic is that such a transmission spectrum is rapidly obtained for a quantum dot array with just a few unit

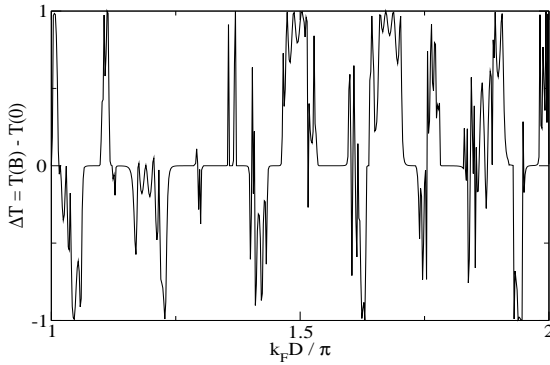


FIG. 2: Magnetically controlled flow demonstrated via the profile of the difference of the quantum transmission for the field-free and $B = 0.3B_c$ cases.

cells as can be seen from the comparison of the upper and lower panels of Figs. 1(b) and 1(c). In practice, this facilitates the realization of a device at length scales comparable to the electronic phase coherence length at finite temperatures so that quantum features do not wash out. The fast convergence of the transmission with length has been previously observed in conductance investigations of oligomer-based molecular junctions [18]. Here, however, in a trade-off with the typical linear dimension of the device it is possible to apply moderate magnetic fields in order to manipulate the electric response; for the same magnetic flux Φ through the dot, the larger W is, the smaller the magnetic field needs to be since $\Phi = BW^2$.

In Fig. 2, we plot the transmission function difference between the field-free structure and that at a field of strength $B = 0.3B_c$. The positive and negative parts reflect the newly formed magnetic subband structure of Bloch electrons in the corresponding one-dimensional artificial crystal which cause the bright and dark transport windows to occur at different spectral positions. As discussed later, for a given geometry and Fermi energy (i.e., fixed $k_F D/\pi$) the contrast in current flow due the differing transmission spectra can also be traced as a function of magnetic field to yield the evolution of the magnetic subbands. We note that there exists broad energy ranges over which bright transport windows at non-zero magnetic field overlap with dark areas at vanishing B , e.g., at $k_F D/\pi \approx 1.5$ and $k_F D/\pi \approx 1.67$. This feature marks a mechanism for magnetically controlled current flow which can be realized at liquid nitrogen temperatures and above as shown below.

At this point it is instructive to interpret the system of natural units to SI units. Assuming $\lambda_F = 30\text{nm}$ with $m^* = 0.05m_e$ yields $E_F = 33\text{meV}$ and $B_c = 1.68\text{T}$. Regarding dimensions each quantum dot should be $W \approx 75\text{nm}$ wide and the width of the lead $D \approx 22\text{nm}$ at $k_F D/\pi \approx 1.5$. The lattice spacing L is around 100nm defining a total array length of less than 500nm for five coupled-dots. In a strict sense, these dimensions define

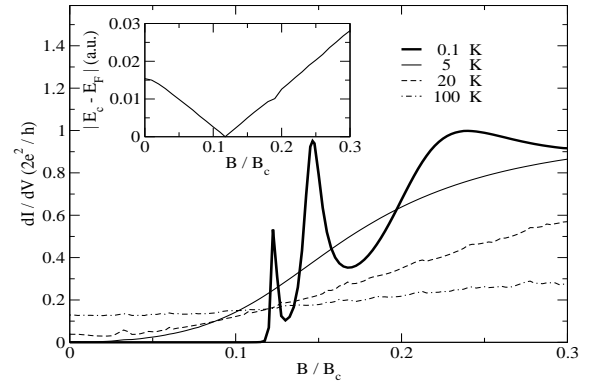


FIG. 3: Linear-response magnetoconductance at various temperatures ($k_F D/\pi \approx 1.5$). Inset: magnetic field dependence of the distance between the Fermi energy $E_F = 74.5\text{meV}$ and the band edge E_c accounting for the resonant structure of the low-temperature magnetoconductance when crossing occurs at $B \approx 0.12B_c \approx 0.45\text{T}$.

TABLE I: SI units at $k_F D/\pi = 1.5$ assuming $m^* = 0.05m_e$.

$\lambda_F(\text{nm})$	$W(\text{nm})$	$E_F(\text{meV})$	$B_c(\text{T})$
20	50	74.5	3.78
30	74	33	1.68
50	123	11.9	0.6

the range of validity of our results regarding temperature. Apart from the thermal broadening, the temperature controls the scattering mechanisms determining the electronic phase coherence length. Since we have so far assumed that electrons are coherently propagating, the array length must be shorter than the latter. More examples are presented in Table I. These show the interplay between linear dimensions and B_c .

In Fig. 3, we furnish our observations with the linear-response magnetoconductance curve at various temperatures. An overall increase of the conductance with magnetic field strength is clearly observed. A remarkable feature is the fine peak-structure of the magnetoconductance dI/dV at very low temperatures which is a consequence of the formation of the spectrum of Bloch electrons in a magnetic field. This is demonstrated in the inset of Fig. 3. As the band structure modifies with the magnetic field, the edge of a single band E_c crosses the Fermi energy E_F at $B/B_c \approx 0.12$. When the distance $|E_c - E_F|$ vanishes a bright transport window is induced that gives rise to the resonant structure of dI/dV in the sub-Kelvin regime (thick line in Fig. 3). Due to the well-pronounced peaks one could think of using these as a probe for the magnetic subband structure. At higher temperatures thermal broadening causes averaging over a larger part of the spectrum including many adjacent minibands and gaps. This increases the low-field conductance whereas simultaneously decreases the correspond-

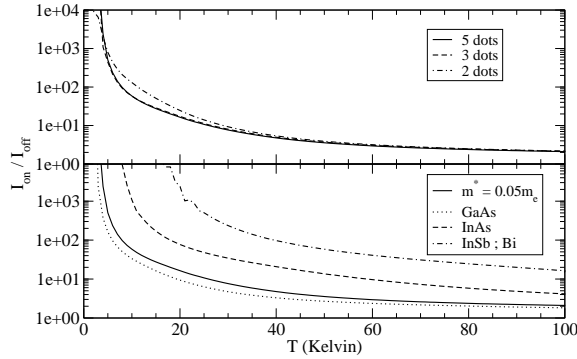


FIG. 4: (Upper panel) Ratio I_{on}/I_{off} of the current flow in the on ($B = 0.3B_c \approx 1.13T$) and off ($B = 0$) state as a function of temperature for an array of $N = 2, 3, 5$ coupled-dots. (Lower panel) Temperature dependence of the I_{on}/I_{off} ratio for various materials parameterized by m^* . $k_F D/\pi$ and E_F are the same as in Fig. 3.

ing higher field values.

A significant quantity in our design is the enhancement (on) - suppression (off) ratio of current flow I_{on}/I_{off} in the linear response regime. In what follows, we analyze its typical behavior heading towards finite temperatures for various materials parameterized via the effective mass by fixing $k_F D/\pi \approx 1.5$. In the upper panel of Fig. 4, the temperature dependence of the I_{on}/I_{off} ratio is shown for an array with varying number N of coupled-dots. Remarkably enough the results hardly modify with $N \gtrsim 3$ in support of our previous remarks. We observe that relatively large ratios in excess of 100 can be achieved for temperatures up to $\sim 10K$ and can be preserved to $I_{on}/I_{off} > 10$ for temperatures up to $\sim 26K$. Further temperature increase makes the ratio to decay smoothly to $I_{on}/I_{off} = 2$ at room temperature. Note that this behavior may be drastically improved with a selective choice of materials and geometry. A search in the parameter space for the latter is best done with an exhaustive analysis of the calculated magnetic subband structure at each field value which is beyond the scope of this Letter. Rather, in the lower panel of Fig. 4 we show how the effective mass of common materials can be readily used in order to considerably improve the device operation since I_{on}/I_{off} ratios magnify at all temperatures as m^* decreases. Notably, for $m^* = 0.01m_e$ (InSb;Bi), $I_{on}/I_{off} > 100$ can be obtained up to $\sim 50K$ and rather enhanced $I_{on}/I_{off} > 10$ can be preserved for temperatures up to $\sim 100K$.

To summarize, we have presented an investigation of ballistic transport through a finite array of coupled-dots from the perspective of a quantum mechanical magnetically tunable mechanism that redefines bright and dark transport windows. The latter have been respectively identified as the energy bands and gaps of the electronic structure of the corresponding one-dimensional artificial crystal despite the small number of dots. Thus, by trac-

ing their magnetic field dependence we showed that the precursor of magnetic subband formation in the energy spectrum can be readily observed. The broad energy range of the transport windows also reveals a well defined mechanism that yields magnetically controlled currents with large enhancement - suppression ratios which can extend up to several tens of Kelvin depending on material parameters. With present technology such a device can be realized within a region of ~ 300 nm at a magnetic field of $\sim 0.5T$.

The authors are grateful to J. Eroms and I. Knezevic for their critical reading of the manuscript and fruitful comments. P. S. D. acknowledges financial support from the Deutsche Forschungsgemeinschaft in the framework of the International Graduiertenkolleg IGK 710. G.F. is thankful to the Science Foundation Ireland for funding.

* Electronic address: panos@tc pci.uni-heidelberg.de

† Electronic address: gfagas@tyndall.ie

‡ Electronic address: peter@tc pci.uni-heidelberg.de

- [1] Y. Alhassid, Rev. Mod. Phys. **72**, 895 (2000).
- [2] S. M. Reimann and M. Manninen, Rev. Mod. Phys. **74**, 1283 (2002).
- [3] L. P. Kouwenhoven, D. G. Austing, and S. Tarucha, Rep. Prog. Phys. **64**, 701 (2001).
- [4] A. M. Chang, H. U. Baranger, L. N. Pfeiffer, and K. W. West, Phys. Rev. Lett. **73**, 2111 (1994).
- [5] R. Akis, D. K. Ferry, and J. P. Bird, Phys. Rev. Lett. **79**, 123 (1997).
- [6] I. H. Chan, R. M. Clarke, C. M. Marcus, K. Campman, and A. C. Gossard, Phys. Rev. Lett. **74**, 3876 (1995).
- [7] S. Oberholzer, E. V. Sukhorukov, C. Strunk, C. Schönenberger, T. Heinzel, and M. Holland, Phys. Rev. Lett. **86**, 2114 (2001); S. Oberholzer, E. V. Sukhorukov, C. Strunk, and C. Schönenberger, Phys. Rev. B **66**, 233304 (2002).
- [8] M. G. Vavilov, L. DiCarlo, and C. M. Marcus, Phys. Rev. B **71**, 241309(R) (2005).
- [9] J. Zak, Phys. Rev. **134**, A1602 (1964); J. Zak, Phys. Rev. **134**, A1607 (1964).
- [10] E. Brown, Phys. Rev. **133**, A1038 (1964).
- [11] D. R. Hofstadter, Phys. Rev. B **14**, 2239 (1976).
- [12] C. Albrecht, J. H. Smet, K. von Klitzing, D. Weiss, R. Hennig, M. Langenbuch, M. Suhrke, U. Rössler, V. Umansky, and H. Schweizer, Phys. Rev. Lett. **86**, 147 (2001).
- [13] R. R. Gerhardts, D. Weiss, and U. Wulf, Phys. Rev. B **43**, R5192 (1991).
- [14] M. Langenbuch, M. Suhrke, and U. Rössler, Europhys. Lett. **61**, 520 (2003).
- [15] J. F. Song, Y. Ochiai, and J. P. Bird, Appl. Phys. Lett. **82**, 4561 (2003).
- [16] M. Elhassan, R. Akis, J. Bird, D. Ferry, T. Ida, and K. Ishibashi, Phys. Rev. B **70**, 205341 (2004).
- [17] P. S. Drouvelis, P. Schmelcher, and P. Bastian, J. Comp. Phys. **215**, 741 (2006).
- [18] G. Fagas, A. Kambili, and M. Elstner, Chem. Phys. Lett. **389**, 268 (2004).